



Cite this: *Analyst*, 2023, **148**, 2657

# Capillary-driven microfluidics: impacts of 3D manufacturing on bioanalytical devices

Pooya Azizian, <sup>a,b</sup> Jasmina Casals-Terré, <sup>b</sup> Jordi Ricart<sup>a</sup> and Joan M. Cabot <sup>\*a</sup>

Over decades, decentralized diagnostics continues to move towards rapid and cost-effective testing at the point-of-care (POC). Although microfluidics has become a key enabling technology for POC testing, the need for robust peripheral equipment has been a key limiting factor in reaching an ideal device. Manufacturing technologies are now reaching a level of maturity that allows the definition of 3D features down to the sub-millimeter scale. Employing three-dimensional (3D) features and surface chemistry allows the possibility to pre-program sophisticated control of the capillary flow avoiding bulky peripheral equipment. By designing a sequence of steps, like elution of reagents, washing, mixing, and sensing, capillary valves have become a powerful tool for POC applications. These valves use capillary force to stop and then release flows within pre-programmed capillary circuits without any moving part. Without their 3D structure, the feasibility of creating pre-programmed bioanalytical devices would be nearly impossible. Besides, the advent of smart materials and their variety of surface properties permitted the unprecedented ability to fabricate reliable flow control with a range of capillary driving forces. The classification of such capillary elements is presented in two functional steps – stop and actuation. This review includes the advances in 3D microfabrication, design, and surface chemistry for manufacturing bioanalytical devices. These developments are critically reviewed, focusing on the process and considering phenomena such as timing, reproducibility, unwanted diffusion, and cross-contaminations.

Received 19th January 2023,  
Accepted 15th April 2023

DOI: 10.1039/d3an00115f

rsc.li/analyst

## 1. Introduction

Microfluidics rapid advances have empowered the demanded applications in sectors like biotechnology, healthcare, and material science, producing essential tools to these fields.<sup>1</sup>

<sup>a</sup>Energy and Engineering Department, Leitat Technological Center, Terrassa, Barcelona, Spain. E-mail: jmcabot@leitat.org

<sup>b</sup>Mechanical Engineering Department, Technical University of Catalonia, Terrassa, Barcelona, Spain



Pooya Azizian

Pooya Azizian has been a PhD student in mechanical engineering (fluid mechanics) at Universitat Politècnica de Catalunya (Barcelona Tech) and a researcher in the Diagnostic Devices Group at LEITAT Technological Center (Spain) since 2020. His PhD is focused on microfluidics for biosensing. He received BSc and MSc in Mechanical Engineering in his hometown, Iran. He joined LEITAT under Marie Skłodowska

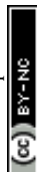
Curie European Training Network (MSCA-ITN-ETN). During the program, he has collaborated with multiple research institutes across Europe involved in BORGES – Biosensing with Organic Electronics project.



Jasmina Casals-Terré

Jasmina Casals-Terré received the MS degree in Mechanical and Aerospace Engineering from the University of California, Irvine, in 2002 and in 2007 a PhD in MEMS switches. She joined the Faculty of Universitat Politècnica de Catalunya-Barcelona Tech where she has established the microfluidics research group, focusing on particle separation with applications in medical diagnosis, optimized tribology and also

MEMS design. She has more than 15 years of experience in research project management and she has authored more than 35 peer-reviewed. She holds several patents (some have been licensed and with international extension).



Microfluidics is both the science of fluid flows and transport phenomena on the micro-scale, and the technology of fluidic systems using microchannels, typically on 10–100 micrometers, to manipulate small amounts of samples and reagents. Microfluidic devices exploit the physical and chemical properties of liquids and gases. Miniaturization offers various advantages over the conventional sized equipment, like the benefit for fewer volumes, high resolution and rapid analysis, cost-effectiveness, and small footprints for the analytical devices.<sup>2</sup> Microfluidics technology also sizes down the equipment that is needed for point-of-care (POC) applications. However, the requirement to use accurate peripheral equipment, like pumps, flow resistors, and electrical valves, to control fluids within microfluidic devices is a limiting factor. Bulky peripheral equipment can be avoided using passive fluid control based on capillary action to accelerate or reduce the velocity of the flow, or even stops it.<sup>3</sup>

Capillary-driven microfluidics usually has different elements, such as inlets, vents, reservoirs, reaction chambers, detection sites, flow resistors, capillary pumps, and capillary valves.<sup>3</sup> An inlet is indeed the fluid entrance into a microfluidic chip. A vent is used as a fluid outlet that ensures the air displacement when the liquid moves along a channel or is introduced at the inlet. A reservoir is usually a microchannel with bigger dimensions than the rest of the circuit's microchannels to store an accurate preset volume of liquid. Usually, a chamber within microfluidics is used to deliver reagents or washing solutions for a variety of analytical steps, like an immunoassay or a chemical reaction. A capillary pump is a passive pump that works based on the suction power offered by the capillary action driven by the surface tension and adhesion between the liquid molecules and the confining walls.<sup>4</sup> So, they do not require any external power source or moving component. Once the pump has been filled with

liquid, the driving force is zero and the pumping process stops. Capillary pumps can be categorized based on the utilized medium (porous materials or solid features on tens of micrometers<sup>5</sup>) and should not considerably increase the flow resistance within the circuit.<sup>6</sup> The last, but not the least, are the capillary valves, where the use of surface chemistry and structure allows the control of the capillary flow in microfluidic devices. A capillary valve can stop and re-activate a flow within a microfluidic circuit. These can be categorized by retention or actuation. The retention of capillary flow can be achieved by decreasing the magnitude of the capillary driving force in a microchannel. The actuation normally requires a secondary fluid or an external mechanism (active or passive) to restart the fluid flow. Some external actuations are based on changing the capillarity on the surface. Capillary valves are named differently depending on the work.<sup>3,7,8</sup> To avoid discussion on the nomenclature, we decided to focus on the retention and actuation functions of the capillary elements rather than the categorization based on the names provided in the literature.

The advent of 3D printing permitted the unprecedented ability to fabricate 3D capillary-driven microfluidic chips capable of spontaneously stopping and re-activating multiple fluids without the need for external parts. Also, the capillary effect on multi-material chips with different surface properties has transformed the development of new capillary elements and pre-programmed capillary devices. This new paradigm is driving this technology to new *in vitro* diagnostic tools where the tests are carried outside of the laboratories, with the view of decentralized diagnostics. Only three reviews in the field of capillary-driven microfluidics have been published over the last 5 years. Two of them are focused mainly on 2D capillary elements,<sup>5,9</sup> and the third analyzes the history, fundamental operating principles, limitations, applications, and emerging ideas related to capillarity elements and capillary-based circuits.<sup>3</sup>



**Jordi Ricart**

*Jordi Ricart Campos received the MS degree in Electronic Engineering from the Universitat Politècnica de Catalunya, in 2005 and in 2010 a PhD in Analysis and Applications of Pulsed Digital Oscillators. On 2010 was lead a microelectronic division of Arquimea company focused on new ASICs design for space applications. He joined at technological center Leitat on 2015 as a Principal investigator of Smart system group and from*

*2017 as a area manager of advanced engineering. He has more than 15 years of experience on research project management and leads research consortiums on regional, national and European projects. As investigator he is the author of several peer-reviewed papers and also has patents on sensors fields.*



**Joan M. Cabot**

*Joan Marc Cabot, MSc and PhD in Analytical Chemistry from University of Barcelona. After his PhD, he joined the ARC Centre of Excellence for Electromaterial Science (ACES, Australia) as a Postdoc and Lecturer, and has done short placements at the UoW (Australia) and DCU (Ireland). Since 2018, Dr Cabot has been working as the PI of the Diagnostic Devices Group in Leitat Technological Centre based in Barcelona (Catalonia).*

*Overall, he accrued 15+ years' excellent scientific track record in analytical tools, microfluidics, biosensors and organ-on-chip. He published 30+ papers (H-index 16) with 1500+ citations, and participated in 50+ dissemination activities.*



Alternatively, this review is focused on the recent impacts of 3D microfabrication, particularly additive manufacturing on the capillary elements' functionality. We believe that understanding the functional steps and the physical processes behind the 3D structures is crucial to design new pre-programmed microfluidics. Therefore, the inclusion criterion for papers was the fact that they involved the current trends in 3D elements. This review focuses on a depth study of their capillary-based functions, providing for the first time a clear view of the 3D structure at different working stages. This paves the way for developing new types of bioanalytical tools, surpassing the limitations and remaining crucial problems to today's bioanalytical applications. In our view and based on the availability of more elaborated and cost-effective 3D microfabrication, it is now the time to identify the 3D capillary elements to step up into novel designs. As a result, herein, after describing the concept of capillary action within microfluidics, the retention and the actuation elements of the capillary valves are studied. The former element is divided into the sudden downstream expansion, the sudden upstream constriction, and the change in surface properties (hydrophobic patch). The latter is categorized as the passive and the active actuations. Moreover, fabrication strategies and materials are reviewed. Finally, the impacts of the field on bioanalytical devices are considered before addressing the future perspective of the reviewed scope.

## 2. Capillary action

At the contact line of an immiscible two-phase fluid interface with a solid surface, the surface free energy, which comes from the molecules of the solid surface, provides an adhesive force to attract the liquid molecules to wet the solid surface (Fig. 1). If there is no force against this adhesive force, the liquid spreads as thin as its molecular thickness on the surface (if there is enough solid surface for all the liquid volume). However, the cohesive intermolecular force of the liquid works against the adhesive force and opposes the liquid from extending (Fig. 1a). It also forms a surface tension on the interface that changes the interface curvature, trying to minimize the two-phase interface area. The balance between these forces, which comes from the molecular interactions, is obtained by the changes in the shape of the two-phase interface (*e.g.* liquid droplet shape) and creates the contact angle of the interface with the solid surface (Fig. 1b). When the cohesive force between the liquid molecules is stronger than the adhesive force, the contact angle of the liquid interface with the solid surface increases to more than 90 degrees. When the surface energy is higher, the surface is more hydrophilic, and the contact angle decreases more to balance the forces and stop the spreading of the liquid on the surface. In excess of liquid, a dynamic flow pushes the fluid till an external force, like gravity, stops it before wetting all the surfaces. For instance, an

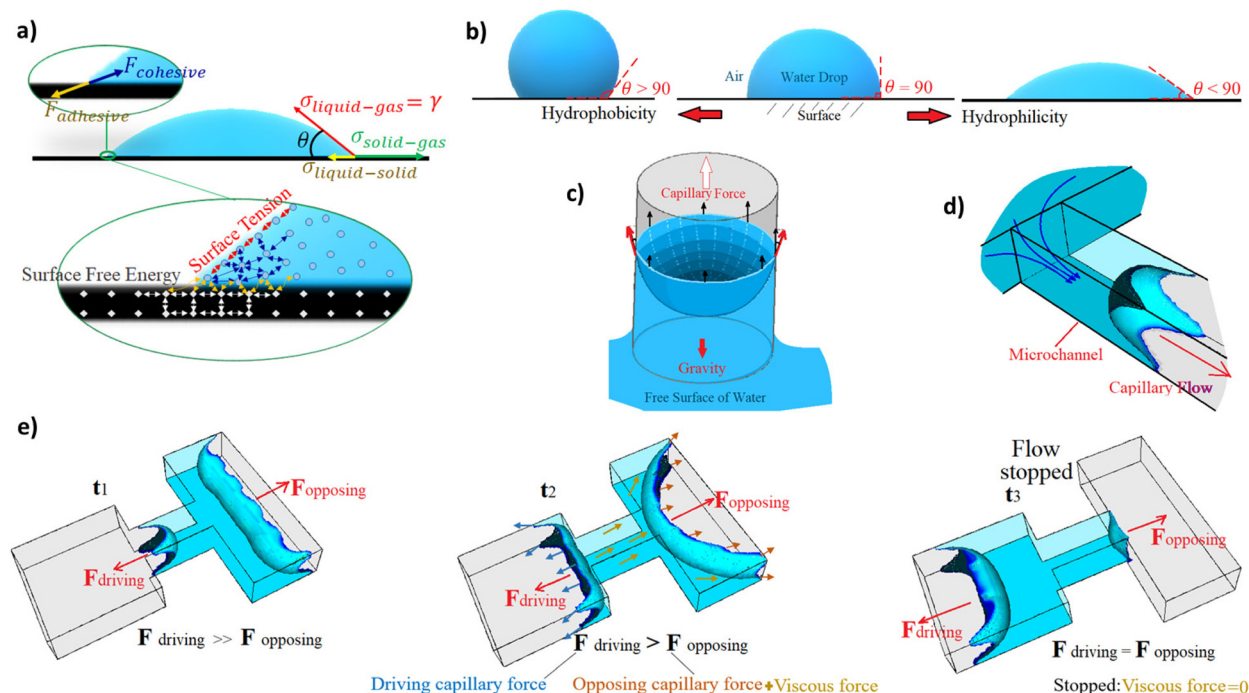


**Fig. 1** Capillary action driven by the hydrophilicity of the surrounding surfaces. (a) Adhesive and cohesive force against each other which leads to drop movement and changing the curvature and contact angle up to the equilibrium by balancing the forces. (b) Change in the contact angle of the aqueous drop by the hydrophilicity of the surface. (c) Capillary action within a narrow tube which drives liquid flow against gravity, and it stops when the capillary force and the weight of the water column become equal. (d) Capillary flow through a microchannel. (e) Capillary flow into the narrow cross-section of the channel empties the liquid from the bigger channel. It continues until the retention opposing pressure at the channel neck stops the drain downstream.



ascending capillary flow in a glass straw (capillary tube) stops in a final state before wetting all the straw's inner surface where the weight of the water column reaches equal to the capillary force (Fig. 1c). On micro-scales, forces like gravity are negligible compared to those from molecular interactions like surface tension. Also, when the confined area that defines/surrounds the fluid pathway is miniaturized, this capillary force scales up because it is applied at the contact perimeter of the liquid and the surrounding walls, and this perimeter becomes more significant relative to the cross-sectional area, where the opposite cohesive force is applied. So, the pressure difference across the interface, called the capillary pressure, increases as the ratio of the applied forces on the surface area increases. Consequently, it drives a higher dynamic flow, named the capillary action, in the hydrophilic microchannels (Fig. 1d). The capillarity-induced pressure, which is the capillary force per unit channel area, is therefore inversely proportional to the characteristics of the channel dimensions. Capillary pressure can work on both directions: either opposing and/or driving the fluid in the channel. It has inverse relation with the curvature of the two-phase interface between immiscible fluids. As a result, the capillary pressure is higher in the thinner tube, leading to stronger capillary driving action or retention opposing pressure (Fig. 1e). Retention opposing pressure is the capillary pressure at the two-phase interface upstream, which works against the driving capillary pressure at the filling front to slow down or stop the capillary drain at the downstream. Capillary-driven microfluidics can be modeled in the conservation of momentum equation as a force just applied on the liquid–gas interface ( $\sigma\kappa\delta_s n$ ) where  $\sigma$ ,  $\kappa$ ,  $\delta_s$ ,  $n$  are the surface tension, curvature, Dirac delta, and the normal vector to the interface, respectively.<sup>10–13</sup>

The capillary pressure can be calculated by employing the Young–Laplace equation.<sup>14</sup> The equation describes the relation between the contact angle, the pressure, the channel size, and the liquid surface tension. The capillary pressure across a liquid–air meniscus in a closed rectangular microchannel can be stated as follows:<sup>15–17</sup>

$$P_{\text{capillary}} = -\sigma \left( \frac{\cos \theta_{\text{top}} + \cos \theta_{\text{bottom}}}{h} + \frac{\cos \theta_{\text{left}} + \cos \theta_{\text{right}}}{w} \right) \quad (1)$$

where  $h$  and  $w$  are the channel height and width, respectively, and  $\theta$  is the contact angle on the different microchannel walls.

If the applied capillary pressures at the two sides of a confined liquid in a capillary structure are balanced, there is no flow. However, when one is bigger than the other, there is a flow from the side with the lower capillary pressure (bigger microchannels – upstream) to the side with the higher capillary pressure (smaller microchannels – capillary pump or downstream). Regarding the viscous force, it is presented against the flow direction (in a dynamic system), and it is defined as the fluid resistance to flow under shear stress. For instance, the shear stress in the  $x$ -direction in the  $x$ - $y$  plane is  $\tau_{xy} = \mu(\partial u/\partial y)$ . This force appears as the viscous term in the

Navier–Stokes equation in 3D space ( $\nabla \cdot (2\mu D)$ , where  $D$  is the deformation tensor). So, considering the deformation tensor, the resistive force against fluid flow is higher in a smaller microchannel than a bigger one. It regulates the flows' velocities and pressure within a capillary channel.

In pre-programmed capillary-driven microfluidics, each of the microfluidic elements are designed based on the capillary pressures and the channel resistances. One of the key elements in capillary circuits is the capillary valves since these features are required to manipulate capillary pressure to stop and reactivate the flow. This principle is achieved by the change of balance between the capillary driving force and the opposing forces. This change can happen, for instance, due to a change in the geometry of the microfluidics. Conventional 2D valves does not offer many options. However, 3D features can employ a broader range of capillary pressures at different sections of an autonomous fluid circuit. When working on 3D, the assembly of multiple valves with distinct geometries becomes a real possibility. The 3D capillary-driven microfluidics can be modeled using an electric circuit analogy, which the capillary pressure at a meniscus works as a source to apply potential.<sup>16,18,19</sup> So that, the electric resistance (representing the fluid resistance) of a filled channel with rectangular cross-sections can be calculated using eqn (2), where  $L$  is the length of the microchannel.<sup>18</sup>

$$R = \frac{12\mu L}{(1 - 0.63(h/w)) \cdot (h^3 \cdot w)} \quad (2)$$

By compiling a series of resistances coming from each capillary elements, it is possible to pre-program sophisticated control of the capillary flow in an autonomous way.

Table 1 summarizes the studies that employed capillary 3D elements and their functions to control and pre-program capillary flow within microfluidic channels.

### 3. Retention elements in 3D capillary-driven microfluidics

Capillary flow can be stopped by passive capillary effects such as the sudden change in the channels' geometry (Fig. 2) or in the surface properties (Fig. 3). In geometry, either the sudden downstream expansion or upstream constriction can stop the capillary flow at the valve's location. In the former, the liquid stops by changing in the meniscus curvature of the filling front. In the latter, the liquid holds in its downstream by providing a retention pressure in the upstream. On some occasions capillary retention is difficult to control due to the variability of the sample such as whole blood, since this retention rely on surface tension and fluid viscosity. However, the geometry can be adapted to create higher retention pressures and increase therefore its reliability. Obviously, a third dimension will increase the number of possibilities in that sense. So, not only the widths of microchannels can be modified, but the depth level can also be changed. Multilevel channels are not





**Table 1** The studies that use 3D capillary elements to control flow within microfluidics in chronological order

| Year (ref.) | Stop stage function   | Actuation stage function  | Min. channel dimension (μm) | Fabrication material & method  | Description  | Application  |
|-------------|---|---|-----------------------------|--|--|--|
| 2002 (15)   | Sudden upstream constriction  | Passive<br>Capillary flow introduced upstream   | Width: 140<br>Depth: 150    | Fabricated in double-side-polished silicon wafer using photolithography and a deep reactive ion etcher. Networks were diced and microcontact-printed on both sides with a flat PDMS stamp. | Autonomous microfluidic capillary-based system in which the introduced reagent drained by capillary pump up to pinning at the capillary retention valve. By introducing the second liquid, it flowed into the closed section and actuated the release of the first liquid.   | The sandwich-type immunoassays like human C-reactive protein detection                                 |
| 2004 (21)   | Sudden downstream expansion   | Passive<br>Capillary flow breaks the interface  | Width: 50<br>Depth: 50      | Patterning a silicon wafer using photoresist; etching the pattern using deep reactive ion etching; dicing the wafer into individual chips and covering with a layer of PDMS.               | Liquid 1 is entered by capillary action and stops at the expanded junction. Then liquid 2 entered and triggered liquid 1 to outlet by making contact at the junction, while it is a bubble-free joining of liquids.  | Timing of independent processes on the same chip; consolidation of multiple samples to a single sample |
| 2006 (22)   | Sudden downstream expansion   | Active<br>Applying burst pressure at upstream   | Width: 30<br>Depth: 15      | Fabricated by a two-level deep reactive ion etching micromachining in a silicon substrate bonded with a PDMS cover.  | The two-level capillary stop valve was presented and studied numerically and experimentally. The expansion of the liquid meniscus with the increase of pressure was depicted. Trigger valves are formed by combining two stop valves. One liquid stops at the junction, then another liquid triggers it and moves forward to the outlet. | Control biological liquids while are less prone to clogging  |
| 2008 (23)   | Sudden downstream expansion   | Passive<br>Capillary flow breaks the interface  | Width: 5<br>Depth: 30       | Fabricated in silicon using photolithography and dry etching.  | Valve stopped the capillary flow by creating a capillary barrier. The barrier was suppressed by gently pressing the valve up to the time that liquid wetted the outlet of the expanded area, and the capillary flow resumed.   | Control the liquid flows for bio-analytical assays like fluorescence sandwich surface immunoassays     |
| 2012 (24)   | Sudden downstream expansion   | Active<br>Press & hold  | Width: 30<br>Depth: 60      | Fabricated both in silicon (UV lithography & deep reactive ion etching) and in plastic (soft lithography & replica molding), also PDMS used for the soft layer.                            | The combination of a trigger valve and a retention burst valve was utilized to encode sequential flow. By reaching the sample to the capillary pump, four different reagents were released based on the required sequence for an immunoassay.  | Reagent control in detecting DNA analytes  |
| 2013 (25)   | First stop: downstream expansion<br>Retention program: sudden upstream constriction | Passive<br>Capillary flow breaks the interface, then reaching the burst pressure to release | Width: 100<br>Depth: 50     | Soft lithography, 2 level molds were fabricated in SU-8, and replicated into PDMS. Air plasma for hydrophilicity. Covered with another PDMS layer.   | Sequential release of reagents for sandwich immunoassays   |  |
| 2016 (18)   | First stop: downstream expansion<br>Retention program: sudden upstream constriction | Passive<br>Capillary flow breaks the interface, then reaching the burst pressure to release | Width: 200<br>Depth: 50     | 3D printed mold using stereolithography printer, and PDMS replication by soft lithography on top of it.  | Sequential liquid delivery for automated biological assays   |  |



Table 1 (Contd.)

| Year (ref.) | Stop stage function                 | Actuation stage function  | Min. channel dimension (μm) | Fabrication material & method  | Description   | Application  |
|-------------|-------------------------------------|---|-----------------------------|--|---|--|
| 2018 (26)   | Sudden downstream expansion         | Passive<br>Capillary flow breaks the interface                                      | Width: 100<br>Depth: 40     | A two-step DRIE (etching) fabricated the valve in silicon.   | A stair-step trigger valve where the junction is deeper provides stable mixing after activation of the valve because liquid from the activated branch flows into both directions at the junction.   | Dilution, mixing, and metering in biochemistry   |
| 2020 (27)   | Sudden downstream expansion         | Passive<br>Capillary flow breaks the interface                                      | Width: 20<br>Depth: 25      | Photolithography and dry etching processes for the silicon microfluidic devices with PEG or APTES coating.   | Study on functionality and surface modification of the stair-step liquid-triggered valve consists of a stop-flow channel and a trigger-flow channel.  | Control of liquid flow at the micro-scale for bioanalytic  |
| 2020 (28)   | Sudden change on surface properties | Active<br>Electrowetting  | Width: 500<br>Depth: 100    | PDMS replica molding using a mold formed with a thick-film photoresist, bonded to glass with PPY printed electrodes.   | An aqueous solution was stopped at the edge of the valve. But changes in the surface state of a film after applying a potential to the valve electrode led to passing the liquid through the valve region.                                      | Controlled solution transport for bioanalysis  |
| 2020 (20)   | Sudden change on surface properties | Active<br>Electrowetting  | Width: 50<br>Depth: 15      | Fabricated on silicon wafer, laser lithography for a photomask, etching the SiO <sub>2</sub> layer, and patterning of metal electrodes using the lift-off process; channels were fabricated by patterning SU8. | Capillary flows stops after reaching the trench by capillary pinning. Then, electrowetting resumes the flow. Activation with different patterns in rows and columns was done by a remote app.   | Remote programmable control and monitoring of flows in biochemical processes   |
| 2021 (29)   | Sudden change on surface properties | Active<br>Electrowetting  | Width: 500<br>Depth: 50     | Pressure-sensitive adhesive was laser cut to fabricate the channel. Nanoparticle-based silver ink was inkjet printed on PET for valve electrodes.  | Skin compatible microfluidic valving system for sweat capture based on electrowetting that changes the surface energy after applying a voltage was presented.   | On-demand sweat capturing to understand the temporal variation of biomarkers   |
| 2021 (30)   | Sudden downstream expansion         | Active<br>A push releases a capillary flow that breaks the interface                | Width: 200<br>Depth: 50     | Using laser cutting of double-sided adhesives to fabrication of lamination-based hollow microchannels.   | The first liquid and the second liquid stop at their junctions. The first valve opens by a mechanical push, and when the first liquid reached the second junction, a single meniscus formed and burst the release of the second liquid as well. | Analytical applications with an accurately controlled concentration  |
| 2021 (31)   | Sudden downstream expansion         | Active<br>Thermo pneumatic actuation by heating up and expansion of the trapped air | Width: 5<br>Depth: 30       | Three deep reactive ion etching steps in silicon, then bonding with glass.   | Electric voltage was provided to heat up and expand the trapped air bubble, and the valve was actuated by breaching the barrier.  | Control the quantity and timing of fluid transport   |
| 2021 (32)   | Sudden downstream expansion         | Passive<br>Capillary flow from downstream in a narrow trigger channel               | Width: 100<br>Depth: 100    | Microchannels were fabricated by micro-milling on PMMA.  | Introduced an off-valve that closes the trigger flow right after triggering the valve array. It prevents backflow in the trigger channel, allowing the supply liquid to be released into the main channel.                                      | Sequential chemical loading for immunoassays while is capable of tuning incubation times and volumes by controlling the flow resistances |



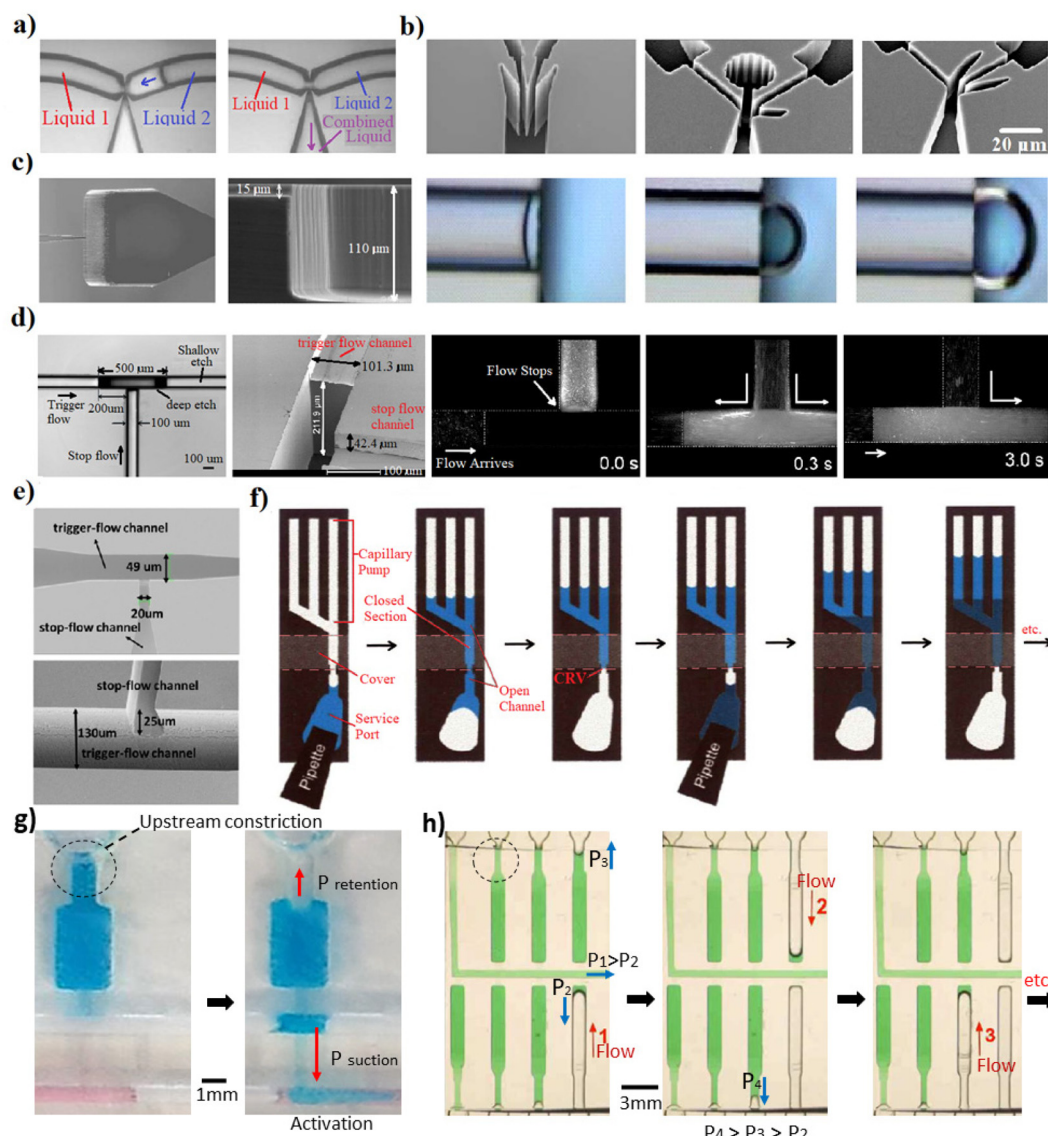
Table 1 (Contd.)

| Year (ref.) | Stop stage function  | Actuation stage function   | Min. channel dimension (μm) | Fabrication material & method   | Description  | Application  |
|-------------|--|--|-----------------------------|---|--|--|
| 2022 (33)   | First stop: downstream expansion retention program: upstream constriction & upstream vent chain action | Passive<br>Capillary flow breaks the interface, then a chain actuation by opening the upstream vents | Width: 250<br>Depth: 100    | Microchannels fabricated by a digital micromirror display (DMD) 3D printer using a transparent resin with customized polymerization exposure time and sealed by adhesive. Also, nitrocellulose membranes were used for the immunoassay. | A microfluidic chain reaction is proposed for the structurally programmed propagation of capillary flow events. Opening the upstream vents relies on evacuating the previous reservoir in an array.                  | Utilized for SARS-CoV-2 antibodies detection in saliva and thrombin generation assay       |
| 2022 (34)   | Sudden downstream expansion & void spacer  | Passive<br>Pneumatic suction created by a capillary-driven mechanism                                 | Width: 500<br>Depth: 100    | Low force stereolithography 3D printing for microchannels and sealed by pressure sensitive adhesive after plasma activation and coating by acrylic acid   | A diffusion-free capillary valve is proposed for pre-programming of liquids' release. A microchannel system works as isolator between reagents till the downstream capillary flow displaces air and opens the valve. | Pre-programmed release of reagents without cross-contamination to perform POC immunoassays |

conventional in microfluidics as the fabrication methods up to date have been limited to the classic 2D soft lithography. So, regardless of whether they are used for the microfluidic mold or the final prototype, the impacts of 3D manufacturing have been pioneering for capillary-driven applications. Besides geometry, surface chemistry within microfluidics can be exploited for the spontaneous manipulation of liquids. Different microfluidic coatings lead to different liquid–solid contact angles. Consequently, distinct capillary pressures or capillary resistances are accessible at different stages. The contact angle, which come from surface chemistry, can be manipulated on the spot by phenomena like electrowetting and can be employed to stop and actuate the capillary flow.<sup>20</sup>

### 3.1. Sudden downstream expansion

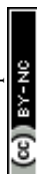
In microfluidics, the abrupt expansion in the downstream geometry eliminates the meniscus curvature or even change the curvature from concave to convex. Consequently, this triggers a significant reduction of the capillary driving force in a microchannel and therefore the retention of capillary flow. This technique has been widely used and certainly it is the most consistent approach to pause capillary flow.<sup>21–23,35</sup> Melin *et al.*<sup>21</sup> proposed a planar junction based on a sudden expansion to stop the flow within one of the connected branches until another capillary flow breaks the meniscus at the junction (Fig. 2a). Later, M. Zimmermann *et al.*<sup>23</sup> developed planar configurations to increase the productivity and reliability of the stop stage of the valves (Fig. 2b). Despite the number of papers on planar valves, the arrival of sophisticated microfabrication techniques, like 3D printing, allowed the development of multi-level and out-of-plane capillary valves, making them more effective and reliable. Glière and Delattre<sup>22</sup> utilized a two-level capillary stop valve which changes the geometry out of the plane to stop the capillary flow. This design provides an additional expansion in the third dimension, leading to a more reliable stop stage. The study depicts the expansion of the liquid meniscus with the increase of the upstream pressure (Fig. 2c). The valve was created using two-level-deep reactive ion etching micromachined in a silicon substrate and the substrate was bonded with a PDMS cover. In this case, multiple etching processes relies on reaching to multiple depth levels.<sup>36</sup> Furthermore, the authors compared the experimental results with the numerical modeling of capillary valves, based on the solution of the free surface equilibrium equation by the finite element method. The computed values of the burst pressure agrees well with the measurements with experimental data in water samples. 3D downstream expansions were used in capillary valves with different configurations for the stop stage. For instance, the stair-step consists of stop-flow and trigger-flow channels has been utilized (Fig. 2d and e). Zhang *et al.*<sup>26</sup> used a stair-step at a T-shaped junction, where a small section of the channel is deeper than the rest (Fig. 2d). This capillary valve has a more reliable stop stage due to the considerable difference in the depth of the stop channel and the trigger channel. The dimensions of the deep-etch in the trigger channel were set at 500 μm length, 100 μm width, and 212 μm

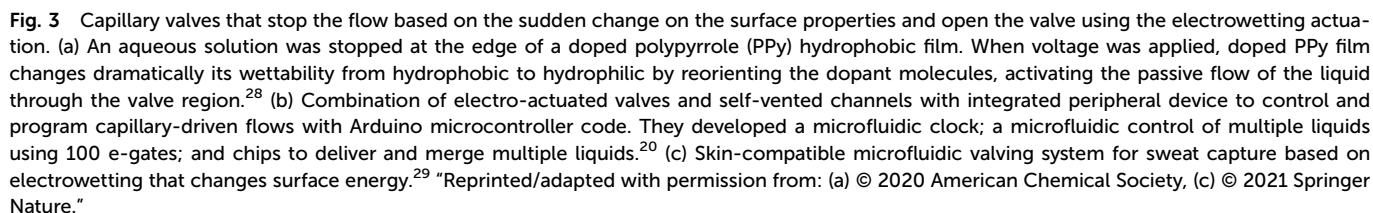


**Fig. 2** Microfluidic studies covering the capillary retention elements designed based on the sudden change in geometry. (a) A planar (2D) trigger valve; the first capillary flow stopped due to the sudden downstream expansion, subsequently the second capillary flow triggered the liquid 1 by making contact at the T-junction. This junction allowed a bubble-free combination of two liquids.<sup>21</sup> (b) Planar configurations of capillary valves that increases burst pressure and therefore the reliability of the stop stage.<sup>23</sup> (c) Two-level capillary stop valve based on the downstream expansion. Expansion of the liquid meniscus.<sup>22</sup> (d) Stair-step trigger valve, where a small portion at the T-junction is deeper. When the valve was triggered, liquid flowed in both directions. Subsequently, backflow stopped, and the mixture flowed into downstream.<sup>26</sup> (e) Two-level stop valve where the flow stopped based on the sudden downstream expansion and was triggered by joining the second capillary flow.<sup>27</sup> (f) Capillary-based system which uses a retention valve to stop the drain of the flow based on the upstream constriction. Joining a capillary flow upstream of the covered section actuates the flow release.<sup>15</sup> (g) Using upstream constriction to retain the flow. The depth of the constricted part is half of the expanded downstream. It is used in combination with complex 3D capillary elements to control the flow.<sup>34</sup> (h) Sudden upstream constriction was utilized to stop the flow and control the retention and release sequence.<sup>18</sup> "Reprinted/adapted with permission from: (a) © 2004 American Chemical Society, (b) © 2008 Springer Nature, (c) © 2006 Elsevier, (d) © 2018 Institute of Physics Publishing, (f) © 2002 American Chemical Society."

depth. Authors demonstrated that this structure provides a limited backflow into the trigger channel up to the step applicable for stable mixing of liquids at the junction.<sup>26</sup> Besides, Chen *et al.*<sup>27</sup> used a T-junction with a deeper trigger channel (130  $\mu\text{m}$  deep and 49  $\mu\text{m}$  wide) with respect to the stop-flow channel (25  $\mu\text{m}$  deep and 20  $\mu\text{m}$  wide). Moreover, Safavieh and Juncker<sup>25</sup> utilized the sudden downstream expansion to stop

the flow (50  $\times$  100  $\mu\text{m}$  stop-flow channel),<sup>18,25</sup> but since it was utilized in combination with the other components to pre-program the flows in capillary circuits, we address the valve function later in more detail. The studies stated above mainly used etching and lithography to fabricate two-level features, which are laborious, time-consuming, and costly. Alternatively, additive manufacturing has open novel approaches for devel-





equal to or higher than 300  $\mu\text{m}$ . Also, downstream expansions with a smoother channel surface and less surface roughness have better performances to keep liquids for a longer time as having lower surface energy. A smooth surface avoids happening of corner flow through sub-micron tracks on the surface. For instance, two directions of 3D-printed features have layer-by-layer structures due to the stepwise additive characteristics of the process; therefore, flow along these edges reduces the valve function in case of low contact angles.<sup>3</sup> Nevertheless, this inconvenient can be avoided by utilizing either abrupt expansion in design, polishing surface, thermal post-processing of surface, or customized layer thickness in the 3D printing process.

### 3.2. Sudden upstream constriction

A constriction in the upstream increases the ratio of the liquid–solid interface perimeter – the contact perimeter of the two-phase fluid interface and the surrounding solid walls – relative to the cross-sectional area where the capillary force is applied on. Thus, it increases retention by opposing capillary force acting against the flow. If this retention force is big enough, it can stop the capillary flow downstream. Juncker *et al.*<sup>15</sup> used this strategy for the first time in 2002 (Fig. 2f) where they produced a 3D upstream constriction valve. In that case, the capillary retention valve was integrated within the microfluidics by covering a section of the open microfluidics, creating a closed microchannel section. The liquid was introduced by a pipette to the open microfluidics and flowed through a closed channel by the capillary action. The liquid drained from the upstream to the capillary pump downstream. It continued till the channel was emptied up to the capillary retention valve and stopped there by the capillary retention of the upstream constriction. By introducing the second liquid, it flowed to the closed section and activated the flow again, draining the liquid downstream. This process can be continued multiple times to introduce different liquids in a sequence. As the suction pressure of the capillary pump is higher than the retention pressure upstream, the fluid flow keeps going. However, as the retention pressure of the valve (covered area) is higher than the suction pressure of the capillary pump, the flow stops at this stage till another liquid joins it to break the retention pressure. Also, other studies used the upstream constriction to stop the flow (Fig. 2g and h),<sup>18,25,34</sup> mostly in combination with the other components to achieve a pre-programmed release of fluids. These pre-programming functions using 3D capillary elements are detailed in Section 5 of this review.

### 3.3. Sudden change based on surface properties

When a capillary flow within a hydrophilic channel reaches a spot with a significant change on surface properties, like a hydrophobic area, the liquid undergoes an abrupt change in the curvature at the interface. If this change is high enough, it can stop the flow. Fig. 3 summarizes some of the relevant approaches. Utilizing the hydrophobic patch to stop the fluid flow was reported first time in 2004 when Teflon was used as a highly insulating coating on Indium Tin Oxide (ITO) coated conductive glass.<sup>37</sup> Recent papers use deposition techniques like inkjet printing that allows the deposition of the hydrophobic patches in a convenient and fast method.<sup>38</sup> The electrodes are patterned, for instance, by inkjet printing of conductive silver ink on the targeted surface of the microfluidics. Afterward, the hydrophilic electrode can be reached by treating the patterned silver by ultraviolet light, and the hydrophobic patch can be fabricated by modifying the silver electrode with a hydrophobic monolayer. The modified silver electrode with this monolayer can dramatically change wettability from hydrophobic to hydrophilic under applying a low potential between two electrodes.<sup>39</sup> In 2020, Pramanik and Suzuki<sup>28</sup>

used a polymer film (DBS-doped polypyrrole) in which an aqueous solution was stopped at the edge of the patch. But after applying a potential to the valve electrode, changes in the film surface state led to the liquid passing through the valve region (Fig. 3a). Arango *et al.*<sup>20</sup> used electrowetting phenomenon to stop and re-activate capillary flow with different patterns in rows and columns by a remote app (Fig. 3b). They could stop, move, route, and synchronize multiple liquids where and when desired electronically using scalable micro-fabrication techniques. Naik *et al.*<sup>29</sup> worked on a skin-compatible microfluidic valving system for sweat capture, based on electrowetting that changes the valve section from hydrophobic to hydrophilic (Fig. 3c). The flow can also be stopped by heating up the microfluidic device. This is called a temperature-controlled hydrophilic patch stop. The flow releases when the device is cooled down.<sup>40</sup> Also, applying geometrical changes on a surface patch can be used as a retention element. For example, a study used a micro-hole array perpendicular to the flow direction.<sup>41</sup> It forms a capillary valve where an abrupt change in contact angle slows the fluid flow. Although the stop stage in these works is passive and based on a hydrophobic patch, an active method must actuate the flow. This implies either a manual or electronic system which normally required fast responsive and compact electronic feedback, normally operated at low voltages (<5 V). Other methods like 3D microfluidic valving systems were based on thermo-responsive hydrogels.<sup>42</sup>

## 4. Actuation elements in 3D capillary-driven microfluidics

The appropriate activation methodology comes from the requirements of the bioanalytical assay. Control, duration, mixing, or flow velocity needs could be different based on the type of assay. Therefore, careful consideration of the required steps must be listed to choose the best capillary elements for the process. Capillary forces can be actuated passively by a secondary liquid or actively using different actuators such as electrocapillary, thermocapillary, or even manually. The passive actuation is based on the design and geometry of the microfluidic device, and it does not require peripheral devices. However, it is a challenging approach for those processes that requires precise incubation times or on-demand activation. The external actuators, on the other hand, provide more precise control on the capillary force, but could have limitations like the undesired effects on charges molecules.

### 4.1. Passive actuation

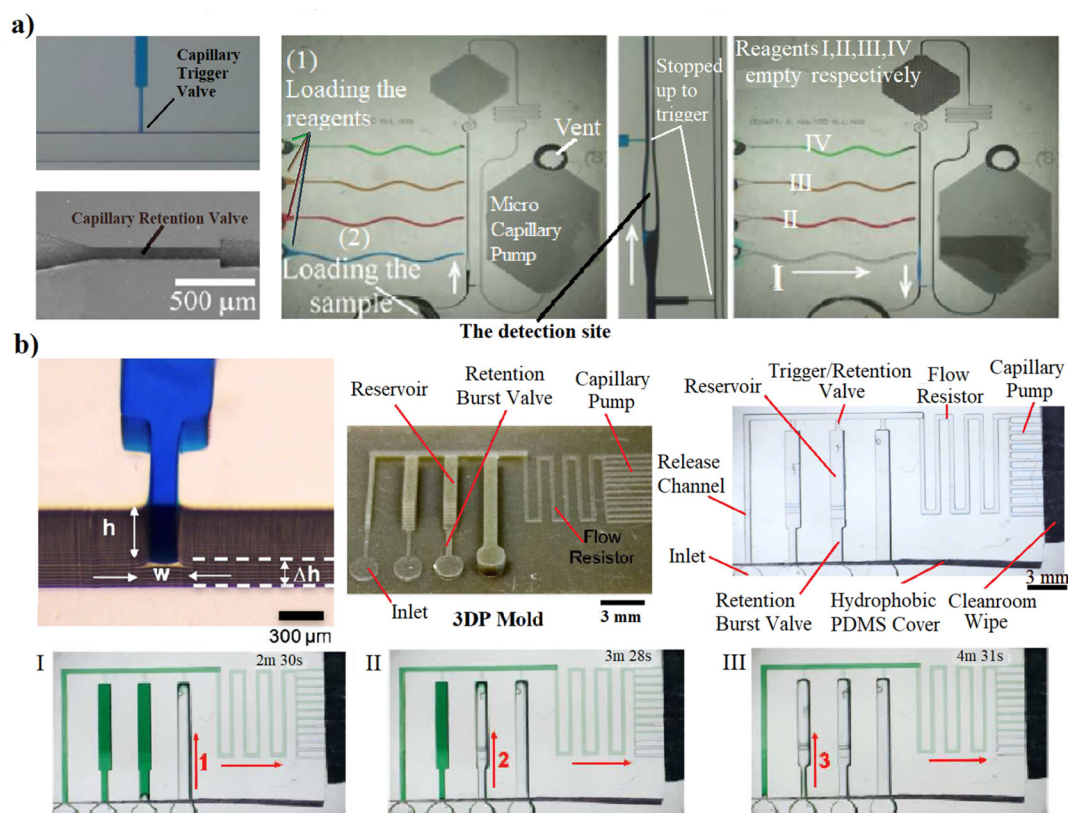
There is at least one actuation step for all capillary-driven microfluidic devices: introduction with another solution or to triggering its release. Passive actuation normally starts with the introducing aqueous solutions at the inlets by a manual action such as pipetting. Then, the liquid flows within the microchannels based on the capillary action regulated by the channel resistances. Multiple automated actuations can be



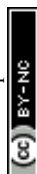
pre-programmed once a capillary flow has been activated. Therefore, the rest of the actuations can happen in a sequence without peripheral instrumentation. Passive actuation is normally used in those designs that incorporate a downstream expansion or upstream constriction. The fluid flow can be planned beforehand based on the dimensions of the microchannels, the surface energy, and the capillary elements. For example, the capillary retention valve based on upstream constriction can be activated when the second liquid joined the first liquid from the upstream. This was demonstrated in the study of an autonomous microfluidic capillary-based system by Juncker *et al.*<sup>15</sup> (Fig. 2f). As soon as the second liquid reaches the first one before the constriction, the curvature of the meniscus breaks, and the two-phase interface is eliminated, which releases the liquid downstream. Alternatively, a triggering liquid can flow across a secondary channel and break the meniscus of a stopped liquid in a sudden downstream expansion area. These valves are named trigger valves as there is both a stop channel and a trigger channel in their configurations. In 2D microfluidic devices, more complex configurations at the junction are required to avoid bubble trapping at the trigger valve while keeping reliable the stop stage (Fig. 2a and b).<sup>21,23</sup> Y-shaped junctions with narrower necking

were utilized with different angles (from 20° to 90°) between the stop channel and the trigger channel. Moreover, opening gaps were used to prevent leakage from the stop channel to empty microchannels before the trigger time. The passive actuation of the multi-level and 3D configurations are similar to the planar trigger valves, except that they activate the stopped flow at the stair-step junctions (Fig. 2d and e).<sup>26,27</sup> When the junction is out of the plane, the design is more reliable and robust, which allows the use of a perpendicular junction instead of more complex configurations. However, the fabrication of multi-level junctions was only feasible in multiple time-consuming and hard-to-reach fabrication steps,<sup>22,25</sup> or certain rapid prototyping fabrication methods introduced lately.<sup>18,33,34</sup>

In some capillary circuits, when passive actuators are used to release liquids, accurate control must be taken for the 2 stages involved during the process: (i) breaking meniscus at the trigger junction by a capillary flow in the main microchannel; (ii) compelling to the retention pressure at the upstream of the stop branch (Fig. 4).<sup>18,25</sup> This idea was utilized to pre-program the fluid release from multiple stop branches (supply channels) in a sequence by allocating specific and different retention pressures for the second stage, which is clarified



**Fig. 4** Passive actuations based on combination of the upstream constriction (retention valves) and the downstream expansion (trigger valves). (a) A passive circuit that encodes sequential activation of 4 solutions. When sample reached the capillary pump, four different reagents were released based on a retention pressure.<sup>25</sup> (b) An autonomous capillary circuit replicated from 3D-printed mold that pre-programmed the reagents' releases by a combination of the trigger valve and the retention burst valve. Releasing liquid from its reservoir happens by reaching the burst pressure at the junction to compel the upstream retention.<sup>18</sup>



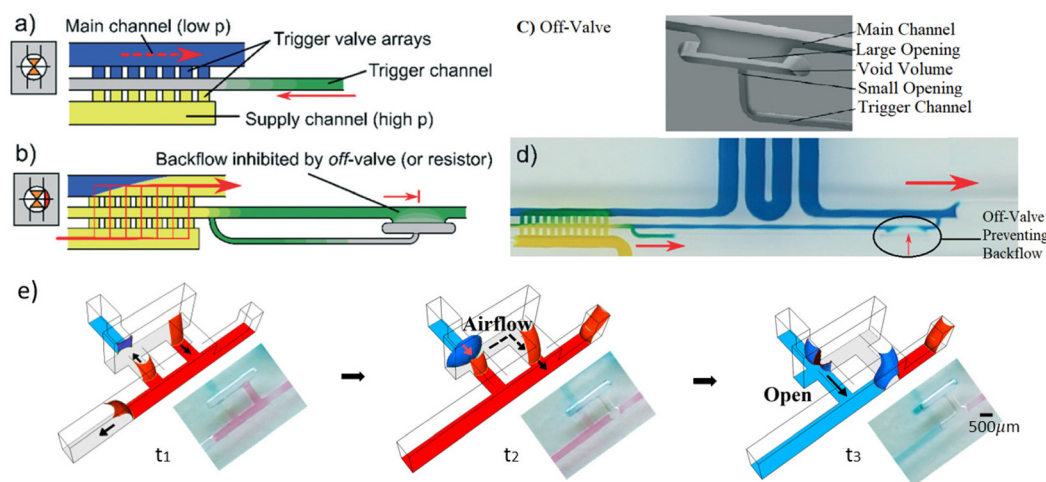


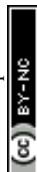
**Fig. 5** Passive actuation avoiding diffusion before the activation using a mediator gap: (a) off-valve was introduced that closes the trigger flow within a mediator-trigger channel right after the event;<sup>32</sup> (b) the array triggered by a mediator channel;<sup>32</sup> (c) off-valve to cut the trigger flow;<sup>32</sup> (d) preventing backflow in the trigger channel by off-valve;<sup>32</sup> (e)  $\pi$ -valve with a void area that acts as an air gap to isolate reagents till pneumatic actuation based on downstream capillary flow and the design configuration opens the valve.<sup>34</sup>

later in the pre-programming section. This method works properly for the programming and the control of the actuation. However, diffusion between the main and supply channels is unavoidable before valve activation. To avoid unwanted diffusion, it is possible to use a trigger channel as a mediator between the main channel and the supply channel(s) (Fig. 5a). In this case, when the trigger channel is empty, the valve is closed due to the sudden expansion, but as soon as the liquid is introduced in this mediator channel, the valve opens. A capillary backflow from downstream of the main channel into the narrower trigger channel can be used to passively activate such a valve. However, the problem of this work is that the liquid in the supply channel prefers to flow through the narrower trigger channel and not into the targeted main channel, due to the higher suction pressure of the downstream in a capillary circuit. Menges *et al.*<sup>32</sup> introduced an off-valve that closes the trigger flow (in the mediator-trigger channel) right after the actuation to prevent unwanted flow into the trigger channel (Fig. 5b–d). In their design, a flow into another channel narrower than the trigger channel push the air into the off-valve section, which cuts the connection of the liquid phase in the trigger channel with the downstream of the main channel.<sup>32,43</sup> Although this design requires precise microfabrication tools, it eliminates unwanted diffusion before the activation time. However, part of the mediator liquid is sacrificed and mixings between solutions can be seen after the activations due to the continuation of the flow from the main channel upstream. Another passive actuation strategy using a mediator channel which avoids unwanted diffusion was proposed by our group (Azizian *et al.*<sup>34</sup>). A void area was introduced between fluids to acts as an air spacer. When the valve is triggered, the air trapped within the void is displaced by a pneumatic suction induced from the capillary flow of the main channel (Fig. 5e). The supply liquid (blue) was actuated when

the liquid in the main channel (red) emptied up to the activation resistance. Since the activation resistance is strong, the capillary pressure in the downstream cannot empty the liquid from the main channel, providing the required suction power to the deep branch (the first branch next to the resistance). Subsequently, the air trapped in the void was displaced by the pneumatic suction introducing the blue into the void and open the valve.

#### 4.2. Assisted actuation

Capillary flow can be activated by external forces like mechanical, electrical, optical, or thermal forces. The greenest approach would be pressing manually and holding up to the filling of the designed chamber, and finally releasing the actuation. This method was used by Hitzbleck *et al.*<sup>24</sup> in which a deformable layer was utilized to fabricate the top covering of the microfluidics (Fig. 6a). Although this method is straightforward and eligible for POC applications, its performance depends on the users so the process could be misused, and its reproducibility questioned. However, due to its simplicity, the idea of using mechanical push has even been utilized lately. In 2021, Jang *et al.*<sup>30</sup> used a multilayer (3D) capillary-driven microfluidics where a manual push introduced a liquid from the top and the bottom layers to the junction of a stop valve based on the sudden expansion in the middle layer (Fig. 6b). This actuation broke the surface tension of the liquid in the middle layer and formed a single meniscus. Then, the fluid was pushed downstream. Up to 7 layers were assembled in this work, taking into account the double-sided adhesives. Glière *et al.*<sup>22</sup> activated the capillary flow by increasing the pressure upstream which finally compels the pressure barrier formed by the convex two-phase interface and release the flow (Fig. 2c). Other activation methods relied on the centrifugal forces, where rotating disks – also known as lab-on-a-disc –



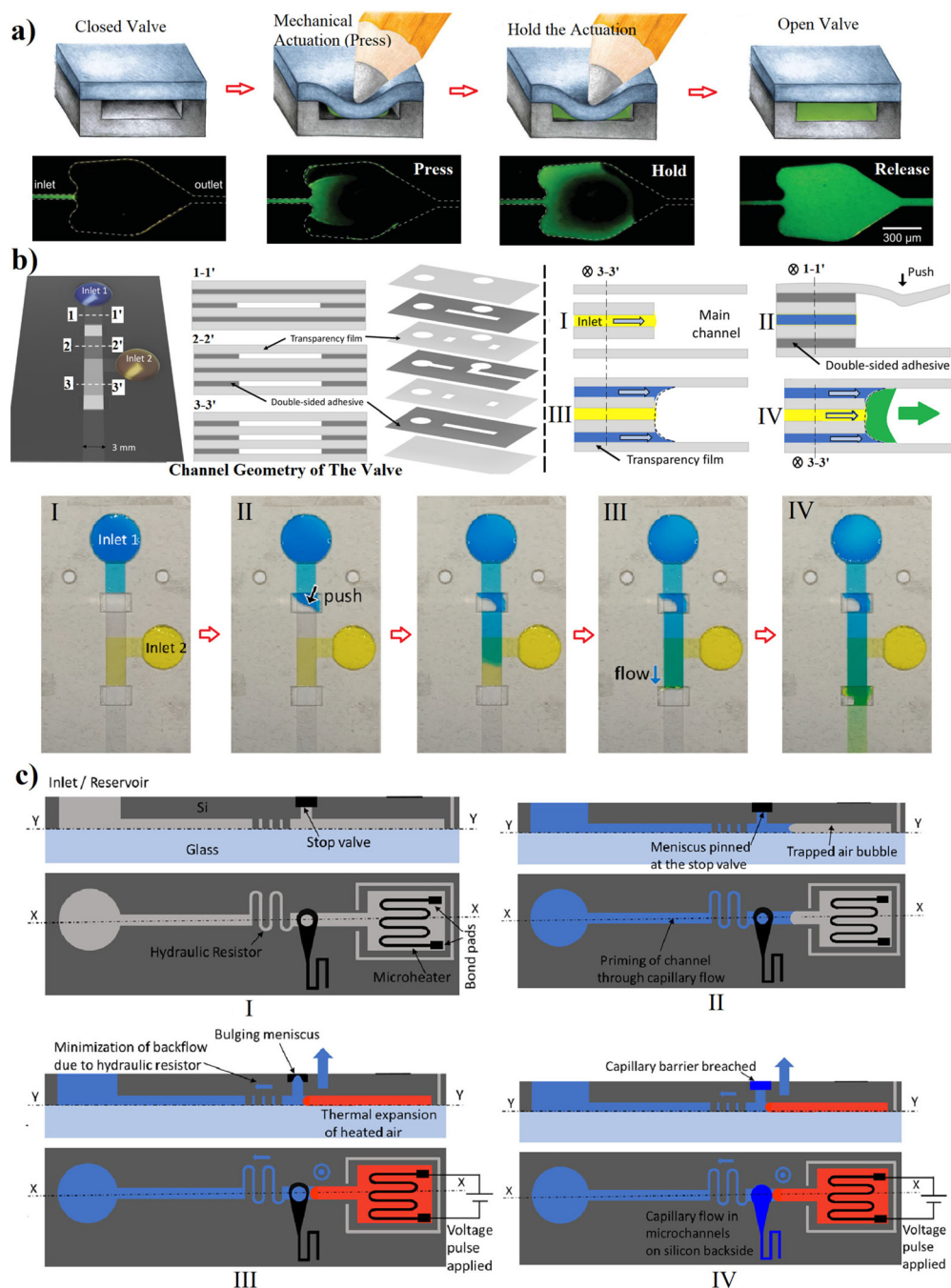


**Fig. 6** Assisted actuation of capillary valves based on: (a and b) manual (mechanical push) actuation,<sup>24,30</sup> and (c) thermo-pneumatic-pressure,<sup>31</sup> it was filled with the capillary flow and waiting to be triggered, a voltage was provided to heat up and expand the trapped air bubble, and valve is actuated by breaching the capillary barrier and capillary flow commences in the microchannel. "Reprinted/adapted with permission from: (c) © 2021 Springer Nature."

were utilized to overcome the capillary stops.<sup>44,45</sup> These kinds of microfluidics require peripheral setups to run with integrated motors, which makes them less attractive for home-testing applications, so we kept them out of the context of this review.

Electrowetting mechanisms offers reliable automation and small instrumentation to control. The hydrophilicity of the

surface can be changed at will by applying an electrical potential. When a capillary flow reaches a hydrophobic patch, it stops there. The contact angle on the hydrophobic path can be changed by applying electrical field and actuate the capillary flow again. This method provides the ability to design complex circuits in which capillary flow can be controlled by a computer or just a mobile application (Fig. 3b).<sup>20</sup> Unknown effects of



charged on biomolecules could affect the movement of certain molecules. Despite the low voltage and current employed, prolonged times may induce undesired electrophoretic mobility or the stacking or depletion of molecules with the opposite charge of the electric field. Besides, the requirements for embedding a supply source (*e.g.*, battery, circuitry) as well as the laborious fabrication protocol might limit their feasibility to be used for single use POC devices. Electrowetting-based valves were firstly used in 2004,<sup>37</sup> and applied for the control of capillary flow three years later.<sup>46</sup> A flexible capillary valve was introduced in 2012.<sup>39</sup> Recently, the redox activity of a DBS-doped polypyrrole (PPy) polymer film was utilized to activate the aqueous flow using  $-0.9\text{ V}$ .<sup>28</sup> Firstly, capillary flow was stopped at the hydrophobic polymer layer. The applied electric potential doped the polymer film, changing its wettability from hydrophobic to hydrophilic by reorienting the dopant molecules (Fig. 3a). These electrodes could be printed (*e.g.* inkjet printing of conductive silver ink) and annealed on flexible substrates like polyethylene terephthalate (PET) and in combination with pressure-sensitive adhesives (PSA) to form controllable valves for the wearable sensors (Fig. 3c).<sup>29</sup>

Activation with ultraviolet (UV) light has also been demonstrated,<sup>47</sup> where 12 W UV lamp at a vertical distance about 10 cm under irradiation at a wavelength of 254 nm was used. This system can also be miniaturized and controlled automatically. However, this approach might not be useful when genetic material or sequences of nucleic acids are considered. Microheaters have also been used to activate fluid flow. Barman *et al.*<sup>31</sup> proposed a capillary valve that was actuated by heating up the trapped air to breach the capillary pressure barrier (Fig. 6c).

## 5. Pre-programmed microfluidic flow

Pre-programming the release of liquids in a capillary circuit is possible when combining multiple capillary 3D elements in strategic positions.<sup>48</sup> This programmed liquid release sequence could be done based on the balance of capillary forces at different sections. Moreover, the flow resistances within microchannels can regulate the flow rates and timings. The resistance and pressure of each capillary element can be determined by eqn (1) and (2). For instance, the actuation of a trigger valve can be pre-programmed by using a combination of a trigger valve with a downstream sudden expansion (to stop the liquid) and a subsequent retention valve with an upstream constriction (to retain the liquid). With the activation of a secondary (supply) liquid stopped at a sudden expansion by a trigger flow, the meniscus in the downstream is removed and so the trigger valve is activated. However, the retention pressure of the upstream constriction (burst valve) retains the release of the liquid till there is enough suction pressure in the downstream to overcome it. A sequence of liquids release from this combination of capillary valves is programmable by the channels dimensions to provide the required retention and suction pressures in a capillary circuit. Thus, by embed-

ding retention valves with different resistances in the upstream, multiple liquids could be released at different intended timing from the less retention power to the highest. The first authors to demonstrate such potential have been R. Safavieh and D. Juncker in 2013<sup>25</sup> as shown in Fig. 4a. First, the capillary flow within the main channel actuated the trigger valves and broke the surface tensions. Then, once the sample reached to the capillary pump, four different reagents were released based on the required sequence for optical detection of the C-reactive protein (CRP). The reagents flow into the main channel only when enough suction pressure is provided to compel the upstream retention pressures of the branch. As these retention pressures were allocated in purpose, they pre-programmed the sequential release of CRP antigen, biotin conjugated detection CRP, washing buffer, streptavidin conjugated Alexa Fluor 488 and finally another washing buffer. The detection of CRP was completed in passive method. Similar concept was followed by Olanrewaju *et al.*<sup>18</sup> with the difference that they used 3D printed molds. The manufacturing of such devices allowed a more practical combination of robust trigger valves and retention burst valves based on the 3D features that could be manufactured (Fig. 4b).

Alternatively, Menges *et al.*<sup>32</sup> introduced in the passive actuation of a sequence of off-valves that switches the flow supply to achieve an automatic and sequential loading of reagents in a capillary circuit. At the pre-programmed time to release each reagent, a capillary flow within a narrower channel from the downstream of the current activated the valve by connecting the supply channel and the main channel. Then the off-valve cut the backflow into the narrower channel. Thus, the new reagent was introduced into the main channel. Using the same approach by integrating more off-valves, flow within a narrow channel from a spot more downward in the capillary circuit, affiliated with an off-valve, activated the release of the next reagent into the circuit (Fig. 7a). Although this valve was utilized within a microfluidic device to measure a relative viscosity,<sup>49</sup> it has the potential to be applied for bio-analytical assays. Moreover, in a recent study, we introduced a pre-programmed capillary-driven microfluidic device, in which a  $\pi$ -valve array was integrated in a capillary circuit for the sequence release of 3 different liquids.<sup>34</sup> The pneumatic suction from a deeper branch triggered sequentially each reagents at the expanded junctions connected to a void area. The supply fluids were released based on their allocated retention pressures (Fig. 7b).

With the compilation of the series of resistances coming from each capillary elements, it is possible to pre-program a cascade of flow events for chain reaction assays. Yafia *et al.*<sup>33</sup> performed such elaborated analytical tasks by proposing a novel microfluidic chain reaction containing a combination of retention and trigger valves with a remarkable difference in the activation function. Until the release of the first reagent is not complete the next one doesn't start because the opening relies on a upstream air vent from the previous chamber. When the first chamber is emptied, there is a way for air to displace into the second chamber, letting the second reagent to



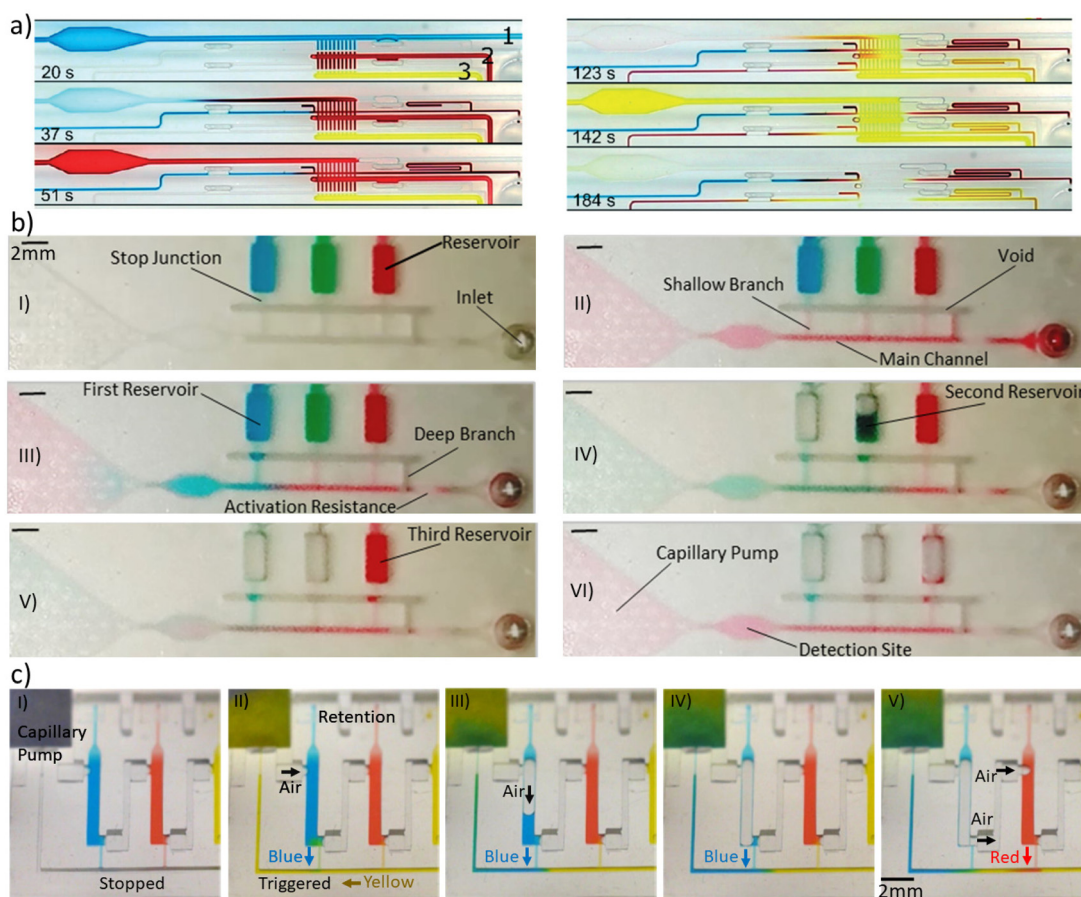


**Fig. 7** Pre-programmed capillary circuits for sequential delivery of liquids. (a) The passive actuation of a sequence of off-valves that switches the flow supply to achieve an autonomous reagents delivery.<sup>32</sup> (b) Pre-programmed flow sequence in a capillary-driven microfluidics based on a series of  $\pi$ -valves.<sup>34</sup> (c) A pre-programmed capillary circuit for a cascade delivery of reagents.<sup>33</sup> The microfluidic chain reaction happens by opening the reservoirs' upstream air vent relied on emptying the previous chamber. "Reprinted/adapted with permission from: (c) © 2022 Springer Nature."

flow downstream. The activation function works like a domino effect (Fig. 7c).

## 6. Fabrication strategies and materials

Various microfabrication methods have been applied for capillary microfluidic studies. Over the years, these methods have been changed from highly time-consuming and challenging (*e.g.* reactive ion etching) to more straightforward and rapid-prototyping techniques (*e.g.* 3D printing). For instance, one of the first microfabrication strategies for pre-programmed capillary flows had numerous fabrication steps: the microfluidic chip was made up on a double-side-polished silicon wafer using photolithography on both sides with a deep reactive ion etcher and connected with a PDMS layer.<sup>15</sup> Recent technologies such as stereolithography (SLA) 3D printing allow rapid fabrication of microfluidic molds containing capillary valves. Furthermore, soft-lithography is easily accessible on top of these molds making is compatible with conventional strate-

gies.<sup>18</sup> Even, direct 3D printing of microfluidic devices is a well-established method. However, to secure a future in microfluidics, printer specifications will need to be improved to enable the fabrication of enclosed microchannels down to 10  $\mu\text{m}$  with minimum roughness, in a range of materials with varying surface properties, and allow for the printing of integrated multifunctional and multi-material devices.<sup>50</sup> Meanwhile, the defects of the 3D printing were minimized in some works using soluble surfactants,<sup>51</sup> adhesive layers,<sup>52</sup> or customized 3D printers by applying different UV exposure times.<sup>33</sup> All in all, additive manufacturing has paved the way to fabricate inexpensive but elaborate parts, as there is no need for expensive facilities like the cleanroom, and the fabrication can be done by transferring the computer-aided design (CAD) file to 3D printers in a distant location. So, in our view, 3D printing will go into the route that the capillary-based devices will be printed directly by 3D printers and not only printing the molds.<sup>33,34</sup>

Another critical issue is the selection of the materials and their surface properties. Generally, capillary circuits require hydrophilic surfaces which drive liquids within the channels



independent from the external forces. The most widely used hydrophilic material in microfluidics is glass because it offers advantages such as transparency, chemical resistance, high pressure, and high thermal conductivity. However, it is costly and extremely challenging to manufacture 3D microfluidic devices.<sup>53,54</sup> For this reason, glass is barely used in point-of-care applications. Cost-effective polymers such as polydimethylsiloxane (PDMS) and poly(methyl methacrylate) (PMMA), are the other prevalent fabrication materials for microfluidics. It is due to some advantages like transparency and biocompatibility. However, PDMS is hydrophobic and, therefore, a surface treatment should be considered in the case of using it. Methods like oxygen or air plasma treatment are applied to generate a bombard of oxygen radicals that oxidize the surface, making it hydrophilic.<sup>18,25</sup> The plasma-treated surfaces are temporarily activated and change back to a hydrophobic surface in some hours. Plasma activation forms reactive silanol functional groups on the surface. So, to solve the lack of the persistency of the hydrophilicity, rinsing the surface into solutions like polyethylene glycol (PEG)<sup>55,56</sup> and polyvinyl alcohol (PVA)<sup>57</sup> can form a hydrophilic coating on the surface. It keeps the treated surfaces hydrophilic for at least weeks.<sup>15,23,26,27</sup> Printing the coating can provide more possibilities to precisely control the flow. For example, aerosol-jet printing was utilized to add a functional coating of PVA to make some targeted microchannels hydrophilic.<sup>58</sup> Besides, fabrication of capillary-driven devices in relatively hydrophilic PMMA needs more expensive thermal process or micromachining as it was done by Menges *et al.* recently.<sup>32</sup> Polymers used in 3D printing, generally called resins, offer a variety of surface properties, but normally suppliers do not provide information about the chemistry of the resins and their activation using plasma or chemical techniques varies from one brand to the other. A good option was published recently where the resin from the SLA from Form3 (Form-labs, USA, clear and black V4 resin) can be activated by vacuum air plasma to make the surface hydrophilic and coated using the acrylic acid fume just after plasma process to increase coating durability (practiced successfully for at least a month).<sup>34</sup> Fabrication of lamination-based hollow microchannels using a laser cutter or xerography is another medium to make capillary valves.<sup>30</sup>

The combination of materials with different surface properties affects the capillary pressure (eqn (1)). Sealing the microfluidic chip with a film with different contact angle can provide robustness for the retention and activation processes in capillary-driven devices. Also, it can be used to avoid the uncontrolled release and failure of the capillary valves using a combination of hydrophobic and hydrophilic surfaces. For instance, Olanrewaju *et al.* sealed the treated PDMS hydrophilic microfluidics with untreated PDMS hydrophobic covers to increase the reliability of the trigger valves in their 3D capillary-driven microfluidics.<sup>18</sup> The combination of materials was also demonstrated by applying lamination for sealing 3DP chips using pressure sensitive adhesives.<sup>33,34</sup> This approach allows the printing lower channels size compared to enclosed

microfluidics chips since we avoid the trapped resins and over-polymerization during printing.<sup>59</sup>

## 7. Impacts on bioanalytical devices

Conventional two-dimensional microfluidics has offered packing lab tasks in single chips requiring fewer samples and reagents, and reducing time, costs and cross-contaminations. However, the requirement for peripheral power and control equipment restricted POC use. For that, 3D capillary-based microfluidics is a pivotal technology toward instrument-less bioanalysis. With a wider library of passive and active components, capillary-driven microfluidic systems can replace monolithically integrated devices and create new opportunities for POC of many bioanalytical applications. In addition, capillary-driven microfluidics systems will benefit significantly from additive manufacturing technologies and smart surfaces, allowing for the further miniaturization of elements and the development of a larger selection of elements and materials. Capillary elements were used to create a number of modular, reconfigurable capillary units containing fluidic and sensor elements, adaptable to many different microfluidic circuits. Sequential release of reagents in 3D capillary-driven microfluidics was used for the sandwich-type immunoassay of human C-reactive protein detection.<sup>15,25</sup> More recently, Yafia *et al.*<sup>33</sup> utilized a pre-programmed 3D capillary microfluidic device to perform chain reaction assay for severe acute respiratory syndrome-coronavirus-2 (SARS-CoV-2) antibodies detection in saliva (Fig. 8a). They also did a thrombin generation assay using a pre-programmed chain reaction by continuous subsampling and analysis of coagulation-activated plasma with parallel operations including timers, iterative cycles of synchronous flow, and stop-flow operations. Such complicated but robust capillary-based circuit demonstrates a clear impact of 3D manufacturing on the POC bioanalytical scope. Another study showed the quantification of urinary protein *via* a colorimetric analysis (Fig. 8b).<sup>60</sup> This study employed a portable smartphone-based detection platform to increase usability and provide a user-friendly alternative. Qu *et al.*<sup>61</sup> presented a POC adalimumab sensor for therapeutic drug monitoring. This biosensor used 3D self-powered microfluidics combined with a fiber optic surface plasmon resonance for the bioanalytical assay. Moreover, 3D-printed microfluidic devices were applied for enzyme-linked immunosorbent assay in which a multistep assay timeline is completed by precisely engineering capillary wetting within printed porous bodies (Fig. 8c).<sup>51</sup> Alternatively, 3D capillary-driven microfluidics were used for other applications like the measurement of dynamic interfacial tension, a difficult parameter to determine due to the instability of two-phase interfaces.<sup>62</sup>

The number of research works that performed bioanalysis through 3DP capillary-driven microfluidics is limited due to the restrictions for controlling surface energy and the difficulty of programming flow without peripheral equipment like pumps and valves. As capillary-driven microfluidics needs



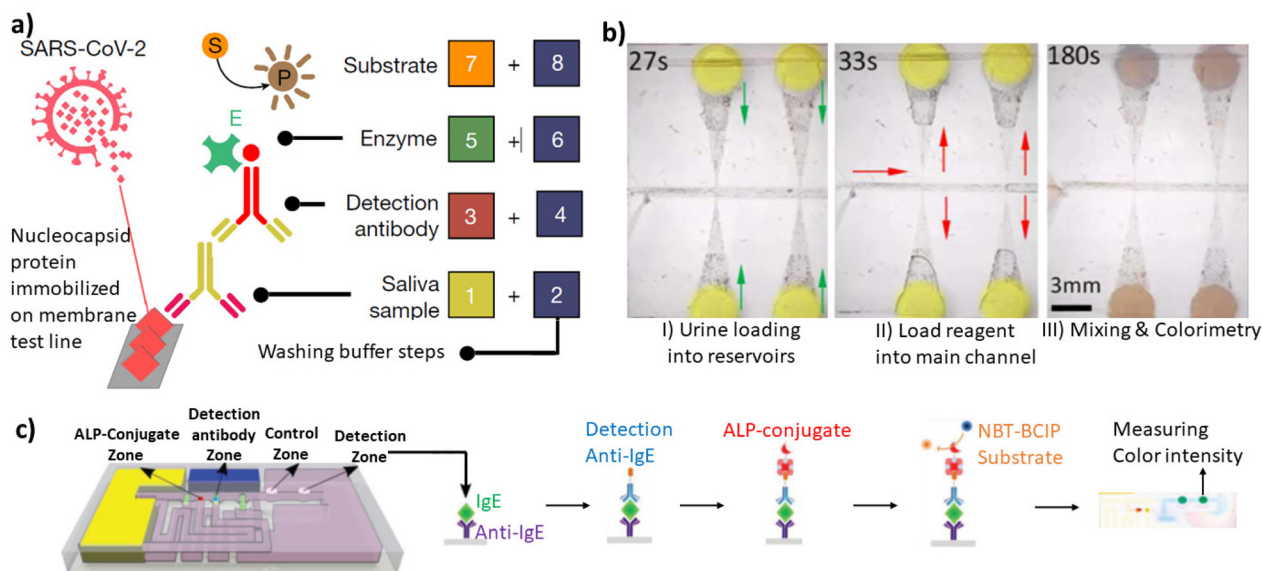


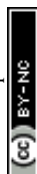
**Fig. 8** Bioanalytical applications of 3D capillary-driven microfluidics. (a) SARS-CoV-2 antibody detection in saliva by the sequential and pre-programmed release of 8 reagents in the capillary 3D circuit.<sup>33</sup> (b) Quantifying the urinary protein via a colorimetric analysis.<sup>60</sup> (c) Autonomous ELISA using IgE, anti-IgE, ALP-conjugate, and NBT-BCIP substrates respectively using a 3D-printed capillary microfluidic device.<sup>51</sup> "Reprinted/adapted with permission from: (b) © 2018 John Wiley and Sons, (c) © 2021 John Wiley and Sons."

sophisticated controlled hydrophilicity on the surfaces of micron-size features, utilizing 3D printing technology for POC bioanalytical applications has been constrained by 3DP materials. However, recently, the studies mentioned earlier used 3DP technologies for bioanalytics by applying novel solutions. In our view, the main reliable utilized strategy is the 3D printing of microfluidics with one open side. Then, it is possible to modify the channels' surface properties from the open side using surface chemistry such as plasma activation or coating mentioned in the previous section. Afterward, closing and sealing microfluidic channels is possible by attaching another layer like a pressure-sensitive adhesive with the required surface energy. On the other hand, sealing a 3DP chip with a clear layer provides better possibilities for optical biosensing. For instance, calorimetry and fluorescent detection of immunoassays are approachable from the side of the clear layer better than the 3DP side, considering that even the 3DP part with a clear resin can still scatter light and reduce the sensitivity of immunosensors.

## 8. Future perspective

3D features have mostly been provided advantages to control capillary flows for autonomous retentions and actuations of microfluidic devices structurally programmed. Capillary action can be used as a source of power to control the flow, in which the capillary retention and actuation elements play a crucial role in applying precise control by stopping and then releasing the reagents on the required time. However, there are some limitations in the microfabrication process and the materials,

as the capillary microfluidics requires specific surface energy to stop and release the fluid flow. Regarding the new fabrication strategies, additive manufacturing has attracted the most attention. Despite the enthusiasm of the early uptakers, its applicability is partially limited by the technical inability to print reliable microfluidic channels with dimensions smaller than hundred micrometers. Despite there is no perfect printer, SLA has been widely used for prototyping such device. Nevertheless, techniques such as microSLA and Two-Photon Polymerization (2PP) are becoming popular due to their ability to produce devices in the meso-scale. 2PP also offer the possibility to incorporate materials such as glass. Having unique capabilities and features when it comes to printing microfluidic devices, the possibilities in the future will result to an increased miniaturization and reliability of the capillary flow. In the matter of perspective materials and surface engineering, we believe that technologies such as the initiator integrated 3D printing (i3DP) has great potential for capillary-based microfluidic devices. The UV-curable resin incorporates a vinyl-terminated initiator, enabling genetic post-printing surface-initiated modification at will.<sup>63</sup> However, commercializing 3DP capillary-driven bioanalytical devices remains a tough challenge because the post-processing step is still time-consuming and costly. So, the technology is mostly used for prototyping. New printing technologies and automated post-processing steps pave the way for new commercial opportunities in the near future. Considering advances in the microfabrication of 3D features and surface chemistry, new capillary elements will be available in a near future. These developments will increase the flow control in terms of speed, retention/activation timing and avoid failure caused by changes in ambient conditions



(humidity and temperature) or contact angle of the surface. Despite this technology is still far from the market, there is room for new advances to exploit their full potential in bioanalytical applications of today's life.

## Author contributions

P. A. did the literature review & data analysis, and wrote the original draft. J. C., J. R. & J. M. C. reviewed & edited the manuscript and supervised the project.

## Conflicts of interest

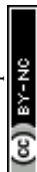
There are no conflicts to declare.

## Acknowledgements

This project has received funding from the European Union's Horizon 2020 research and innovation program under the Marie Skłodowska-Curie grant agreement no. 813863.

## References

- 1 S. Battat, D. A. Weitz and G. M. Whitesides, *Lab Chip*, 2022, **22**, 530–536.
- 2 G. M. Whitesides, *Nature*, 2006, **442**, 368–373.
- 3 A. Olanrewaju, M. Beaugrand, M. Yafia and D. Juncker, *Lab Chip*, 2018, **18**, 2323–2347.
- 4 R. Safavieh, A. Tamayol and D. Juncker, *Microfluid. Nanofluid.*, 2015, **18**, 357–366.
- 5 L. Xu, A. Wang, X. Li and K. W. Oh, *Biomicrofluidics*, 2020, **14**, 031503.
- 6 H. Madadi, J. Casals-Terré, R. Castilla-López and M. Sureda-Anfres, *Microfluid. Nanofluid.*, 2013, **17**, 115–130.
- 7 H. Cho, H. Y. Kim, J. Y. Kang and T. S. Kim, *J. Colloid Interface Sci.*, 2007, **306**, 379–385.
- 8 V. Siljegovic, N. Milicevic and P. Griss, Digest of Technical Papers – International Conference on Solid State Sensors and Actuators and Microsystems, TRANSDUCERS '05, 2005, vol. 2, pp. 1565–1568.
- 9 S. Wang, X. Zhang, C. Ma, S. Yan, D. Inglis and S. Feng, *Biosensors*, 2021, **11**, 405.
- 10 P. Azizian, M. Azarmanesh, M. Dejam, M. Mohammadi, M. Shamsi, A. Sanati-Nezhad and A. A. Mohamad, *Chem. Eng. Sci.*, 2019, **195**, 201–207.
- 11 M. Azarmanesh, M. Dejam, P. Azizian, G. Yesiloz, A. A. Mohamad and A. Sanati-Nezhad, *Sci. Rep.*, 2019, **9**, 6723.
- 12 M. Azarmanesh, M. Farhadi and P. Azizian, *Int. J. Numer. Methods Heat Fluid Flow*, 2015, **25**, 1705–1717.
- 13 M. Azarmanesh, M. Farhadi and P. Azizian, *Phys. Fluids*, 2016, **28**, 032005.
- 14 J. C. T. Eijkel and A. van den Berg, *Lab Chip*, 2006, **6**, 1405–1408.
- 15 D. Juncker, H. Schmid, U. Drechsler, H. Wolf, M. Wolf, B. Michel, N. de Rooij and E. Delamarche, *Anal. Chem.*, 2002, **74**, 6139–6144.
- 16 D. Mikaelian and B. Jones, *SN Appl. Sci.*, 2020, **2**, 415.
- 17 S. Ghosh, K. Aggarwal, T. U. Vinitha, T. Nguyen, J. Han and C. H. Ahn, *Microsyst. Nanoeng.*, 2020, **6**, 1–18.
- 18 A. O. Olanrewaju, A. Robillard, M. Dagher and D. Juncker, *Lab Chip*, 2016, **16**, 3804–3814.
- 19 S. W. Kang and D. Banerjee, *J. Fluids Eng.*, 2011, **133**, 054502.
- 20 Y. Arango, Y. Temiz, O. Gökçe and E. Delamarche, *Sci. Adv.*, 2020, **6**, eaay8305.
- 21 J. Melin, N. Roxhed, G. Gimenez, P. Griss, W. van der Wijngaart and G. Stemme, *Sens. Actuators, B*, 2004, **100**, 463–468.
- 22 A. Glière and C. Delattre, *Sens. Actuators, A*, 2006, **130**, 601–608.
- 23 M. Zimmermann, P. Hunziker and E. Delamarche, *Microfluid. Nanofluid.*, 2008, **5**, 395–402.
- 24 M. Hitzbleck, L. Avrain, V. Smekens, R. D. Lovchik, P. Mertens and E. Delamarche, *Lab Chip*, 2012, **12**, 1972–1978.
- 25 R. Safavieh and D. Juncker, *Lab Chip*, 2013, **13**, 4180–4189.
- 26 L. Zhang, B. Jones, B. Majeed, Y. Nishiyama, Y. Okumura and T. Stakenborg, *J. Micromech. Microeng.*, 2018, **28**, 065005.
- 27 X. Chen, S. Chen, H. Yang and Y. Zhang, *Micromachines*, 2020, **11**, 690.
- 28 S. K. Pramanik and H. Suzuki, *ACS Appl. Mater. Interfaces*, 2020, **12**, 37741–37749.
- 29 A. R. Naik, B. Warren, A. Burns, R. Lenigk, J. Morse, A. Alizadeh and J. J. Watkins, *Microfluid. Nanofluid.*, 2021, **25**, 1–9.
- 30 I. Jang, H. Kang, S. Song, D. S. Dandy, B. J. Geiss and C. S. Henry, *Analyst*, 2021, **146**, 1932–1939.
- 31 U. Barman, L. Lagae and B. Jones, *Microsyst. Technol.*, 2021, **27**, 681–692.
- 32 J. Menges, C. Meffan, F. Dolamore, C. Fee, R. Dobson and V. Nock, *Lab Chip*, 2021, **21**, 205–214.
- 33 M. Yafia, O. Ymbern, A. O. Olanrewaju, A. Parandakh, A. Sohrabi Kashani, J. Renault, Z. Jin, G. Kim, A. Ng and D. Juncker, *Nature*, 2022, **605**, 464–469.
- 34 P. Azizian, J. Casals-Terré, J. Ricart and J. M. Cabot, 2022, PREPRINT (Version 1) available at Research Square, DOI: [10.21203/rs.3.rs-2165436/v1](https://doi.org/10.21203/rs.3.rs-2165436/v1).
- 35 X. Du, P. Zhang, Y. Liu and Y. Wu, *Sens. Actuators, A*, 2011, **165**, 288–293.
- 36 S. K. Ajmera, C. Delattre, M. A. Schmidt and K. F. Jensen, *Sens. Actuators, B*, 2002, **82**, 297–306.
- 37 J. Y. Cheng and L. C. Hsiung, *Biomed. Microdevices*, 2004, **6**, 341–347.
- 38 K. A. Bernetski, C. T. Burkhart, K. L. Maki and M. J. Schertzer, *Microfluid. Nanofluid.*, 2018, **22**, 1–10.



- 39 T. Mérian, F. He, H. Yan, D. Chu, J. N. Talbert, J. M. Goddard and S. R. Nugen, *Colloids Surf., A*, 2012, **414**, 251–258.
- 40 L. Li, E. Y. Westerbeek, J. C. Vollenbroek, S. de Beer, L. Shui, M. Odijk and J. C. T. Eijkel, *Soft Matter*, 2021, **17**, 7781–7791.
- 41 Y. Xie, H. You, Z. Gao, Z. Huang and M. Yang, *Anal. Sci.*, 2018, **34**, 1323–1327.
- 42 H. Lin, J. Tan, J. Zhu, S. Lin, Y. Zhao, W. Yu, H. Hojaiji, B. Wang, S. Yang, X. Cheng, Z. Wang, E. Tang, C. Yeung and S. Emaminejad, *Nat. Commun.*, 2020, **11**, 1–12.
- 43 C. Meffan, J. Menges, F. Dolamore, D. Mak, C. Fee, R. C. J. Dobson and V. Nock, *Microsyst. Nanoeng.*, 2022, **8**, 1–13.
- 44 J. M. Chen, P. C. Huang and M. G. Lin, *Microfluid. Nanofluid.*, 2008, **4**, 427–437.
- 45 A. Kazemzadeh, P. Ganesan, F. Ibrahim, S. He and M. J. Madou, *PLoS One*, 2013, **8**, e73002.
- 46 W. Satoh, H. Yokomaku, H. Hosono, N. Ohnishi and H. Suzuki, *J. Appl. Phys.*, 2008, **103**, 034903.
- 47 T. Guo, T. Meng, W. Li, J. Qin, Z. Tong, Q. Zhang and X. Li, *Nanotechnology*, 2014, **25**, 125301.
- 48 P. Azizian, A. Ortega, J. Ricart, J. Casals-Terré and J. M. Cabot, in 24th International Conference on Miniaturized Systems for Chemistry and Life Sciences, 2020, pp. 164–165.
- 49 R. C. Meffan, J. Menges, F. Dolamore, D. Mak, C. Fee, V. Nock and R. Dobson, *ChemRxiv*, 2021, DOI: [10.26434/CHEMRXIV-2021-W0ZC9](https://doi.org/10.26434/CHEMRXIV-2021-W0ZC9).
- 50 S. Waheed, J. M. Cabot, N. P. Macdonald, T. Lewis, R. M. Guijt, B. Paull and M. C. Breadmore, *Lab Chip*, 2016, **16**, 1993–2013.
- 51 C. Achille, C. Parra-Cabrera, R. Dochy, H. Ordutowski, A. Piovesan, P. Piron, L. van Looy, S. Kushwaha, D. Reynaerts, P. Verboven, B. Nicolai, J. Lammertyn, D. Spasic and R. Ameloot, *Adv. Mater.*, 2021, **33**, 2008712.
- 52 P. Azizian, E. Guerrero-Sanvicente, R. Grinyte, J. Casals-Terré and J. M. Cabot, in 25th International Conference on Miniaturized Systems for Chemistry and Life Sciences, 2021, pp. 1779–1780.
- 53 F. Kotz, K. Arnold, W. Bauer, D. Schild, N. Keller, K. Sachsenheimer, T. M. Nargang, C. Richter, D. Helmer and B. E. Rapp, *Nature*, 2017, **544**, 337–339.
- 54 F. Kotz, P. Risch, K. Arnold, S. Sevim, J. Puigmartí-Luis, A. Quick, M. Thiel, A. Hrynevich, P. D. Dalton, D. Helmer and B. E. Rapp, *Nat. Commun.*, 2019, **10**, 1–7.
- 55 H. P. Long, C. C. Lai and C. K. Chung, *Surf. Coat. Technol.*, 2017, **320**, 315–319.
- 56 C. C. Lai and C. K. Chung, *Surf. Coat. Technol.*, 2020, **389**, 125606.
- 57 T. Trantidou, Y. Elani, E. Parsons and O. Ces, *Microsyst. Nanoeng.*, 2017, **3**, 1–9.
- 58 N. Čatić, L. Wells, K. Al Nahas, M. Smith, Q. Jing, U. F. Keyser, J. Cama and S. Kar-Narayan, *Appl. Mater. Today*, 2020, **19**, 100618.
- 59 N. P. Macdonald, J. M. Cabot, P. Smejkal, R. M. Guijt, B. Paull and M. C. Breadmore, *Anal. Chem.*, 2017, **89**, 3858–3866.
- 60 S. Yan, Y. Zhu, S. Y. Tang, Y. Li, Q. Zhao, D. Yuan, G. Yun, J. Zhang, S. Zhang and W. Li, *Electrophoresis*, 2018, **39**, 957–964.
- 61 J. H. Qu, H. Ordutowski, C. van Tricht, R. Verbruggen, A. Barcenas Gallardo, M. Bulcaen, M. Ciwinka, C. Gutierrez Cisneros, C. Devriese, S. Guluzade, X. Janssens, S. Kornblum, Y. Lu, N. Marolt, C. Nanjappan, E. Rutten, E. Vanhauwaert, N. Geukens, D. Thomas, F. Dal Dosso, S. Safdar, D. Spasic and J. Lammertyn, *Biosens. Bioelectron.*, 2022, **206**, 114125.
- 62 B. Deng, K. Schroën, M. Steegmans and J. de Ruiter, *Lab Chip*, 2022, **22**, 3860–3868.
- 63 X. Wang, X. Cai, Q. Guo, T. Zhang, B. Kobe and J. Yang, *Chem. Commun.*, 2013, **49**, 10064–10066.

